

Title	Complete set of elastic and piezoelectric coefficients of α -quartz at low temperatures
Author(s)	Tarumi, Ryuichi; Nakamura, Koichi; Ogi, Hirotsugu et al.
Citation	Journal of Applied Physics. 2007, 102(11), p. 113508-1-113508-6
Version Type	VoR
URL	https://hdl.handle.net/11094/84226
rights	This article may be downloaded for personal use only. Any other use requires prior permission of the author and AIP Publishing. This article appeared in Journal of Applied Physics, 102(11), 113508 (2007) and may be found at https://doi.org/10.1063/1.2816252 .
Note	

Osaka University Knowledge Archive : OUKA

<https://ir.library.osaka-u.ac.jp/>

Osaka University

Complete set of elastic and piezoelectric coefficients of α -quartz at low temperatures

Ryuichi Tarumi,^{a)} Koichi Nakamura, Hirotsugu Ogi, and Masahiko Hirao

Nonlinear Mechanics Division, Graduate School of Engineering Science, Osaka University, 1-3 Machikaneyama, Toyonaka, Osaka 560-8531, Japan

(Received 17 July 2007; accepted 26 September 2007; published online 6 December 2007)

A complete set of low temperature elastic constants C_{ij} and piezoelectric coefficients e_{ij} of α -quartz single crystal has been investigated by resonance ultrasound spectroscopy coupled with a laser-Doppler interferometry. Most elastic constants showed monotonic elastic stiffening, while C_{66} continuously softened as the temperature decreased. Two piezoelectric coefficients e_{ij} showed monotonic decreasing upon cooling, and we found a strong correlation between e_{11} and C_{66} , representing that thermal contraction induced internal strain plays an important role in their temperature behaviors. Group theoretical lattice dynamics analysis revealed that the elastic softening and the correlation can be attributed to an optical-mode-phonon-type internal strain having doubly degenerated E symmetry in the point group of D_3 . © 2007 American Institute of Physics. [DOI: 10.1063/1.2816252]

I. INTRODUCTION

α -quartz (α -SiO₂) has a trigonal crystal structure with the space group symmetry of $P3_221$ (or $P3_121$ in its chiral pair). Since the discovery of piezoelectric effect by the Curie brothers in 1880,¹ its moderate piezoelectricity, high temperature stability of resonance frequencies, and low internal friction have provided a variety of applications to acoustic devices such as filters, oscillators, sensors, etc. Up to now, intensive measurements on elastic constants C_{ij} and piezoelectric coefficients e_{ij} of α -quartz are carried out.^{1–11} On the other hand, α -quartz undergoes a α - β structural phase transition at high temperature^{12–14} and solid-state amorphization under high pressure.^{2,15–17} Being related to these phase stability of α -quartz, evaluations of higher-order elasticity,¹⁸ negative Poisson's ratio,¹⁹ lattice vibrations,^{20,21} and internal frictions¹¹ are also interesting issues.

Independent studies^{11,15} showed that currently used C_{ij} and e_{ij} of α -quartz are inconsistent with each other even at ambient temperature. Needless to say, the disagreement becomes marked about their temperature dependences.¹ A part of this origin can be attributed to the experimental procedure; previous methods require many independent measurements for different crystals and need to solve simultaneous equations. In addition, they include various measurement errors due to crystal misorientations, resonance-frequency shift by attached electrodes and coupling agents, ambiguous electric boundary conditions, etc.¹¹ Resonance ultrasound spectroscopy (RUS) is a state of the art technique because it simultaneously determines both C_{ij} and e_{ij} from only one single crystal specimen with high accuracy.^{22–26} Recently, Ogi *et al.* reinvestigated C_{ij} and e_{ij} of α -quartz by the RUS coupled with a laser-Doppler interferometry (RUS/LDI) and provided a reliable result at ambient temperature.^{11,26} However, low temperature measurements have not been performed by the method. Generally, elastic constants C_{ij} are defined as the

fourth-rank coefficient tensor to the second derivative of internal energy with respect to Lagrange strains; a complete set of low temperature C_{ij} is therefore, indispensable to derive an accurate thermodynamic equation of state. Furthermore, both low temperature C_{ij} and e_{ij} are required to account for the theoretical calculation accuracies, such as density functional *ab initio* studies and lattice dynamics calculations,^{15,21} as well as most research works mentioned above.

Motivated by the current status, we investigated the complete set of elastic constants C_{ij} and piezoelectric coefficients e_{ij} of the α -quartz single crystal by the RUS/LDI method from ambient temperature to 5 K. The first-order temperature coefficients of elastic constants showed quantitative agreements with previous values supporting the accuracy of the present study. C_{66} and e_{11} continuously decrease as the temperature decreases and are found to show a strong correlation with each other; the Pearson product-moment correlation coefficient becomes 0.98, which is remarkably close to unity. The origin of softening of C_{66} and the strong correlation with e_{11} have been discussed on the basis of a group theoretical lattice dynamics approach.²⁷

II. EXPERIMENTAL PROCEDURE

A. Material

The material studied is a $4.8 \times 5.2 \times 5.8$ mm³ rectangular parallelepiped right-handed α -quartz ($P3_221/D_3^5$) single crystal cut along crystallographic X , Y , and Z orientations. The accuracies of size and orientations are ± 1 μ m and $\pm 1^\circ$, respectively. Mass density ρ determined from the dimension and mass of the specimen is $\rho = 2643.51$ kg/m³, which is almost consistent with the x-ray result ($\rho = 2648.6$ kg/m³).²⁸ α -quartz has a threefold screw axis along the $[0, 0, Z]$ direction and three twofold rotation axes within the X - Y plane. It includes three SiO₂ molecules in a unit cell; the O atoms are located at the 6c Wyckoff position (general position) and Si

^{a)}Electronic mail: tarumi@me.es.osaka-u.ac.jp.

atoms are located at the $3b$ position. As a result, it is constructed from SiO_4 tetrahedra sharing their $6c$ corners with each other.

According to the point group of D_3 , α -quartz has six independent elastic constants C_{ij} and two piezoelectric coefficients e_{ij} ,

$$C_{ij} = \begin{bmatrix} C_{11} & C_{12} & C_{13} & C_{14} & 0 & 0 \\ C_{12} & C_{11} & C_{13} & -C_{14} & 0 & 0 \\ C_{13} & C_{13} & C_{33} & 0 & 0 & 0 \\ C_{14} & -C_{14} & 0 & C_{44} & 0 & 0 \\ 0 & 0 & 0 & 0 & C_{44} & C_{14} \\ 0 & 0 & 0 & 0 & C_{14} & C_{66} \end{bmatrix}, \quad (1)$$

$$e_{ij} = \begin{bmatrix} e_{11} & -e_{11} & 0 & e_{14} & 0 & 0 \\ 0 & 0 & 0 & 0 & -e_{14} & -e_{11} \\ 0 & 0 & 0 & 0 & 0 & 0 \end{bmatrix}. \quad (2)$$

Here, $C_{66} = (C_{11} - C_{12})/2$. The superscript E for C_{ij} is abbreviated for simplicity. In addition to C_{ij} and e_{ij} , it has two dielectric coefficients ε_{ij} . In this work, we fixed the $\varepsilon_{11}/\varepsilon_0$ and $\varepsilon_{33}/\varepsilon_0$ to be 4.424 and 4.632 (Ref. 11) since the reported temperature coefficients of ε_{ij} are less significant compared with e_{ij} about one to two orders in magnitude.¹

B. Resonance ultrasound spectroscopy

The free vibration resonance frequencies of a specimen depend on dimensions, mass density, and independent material constants of C_{ij} , e_{ij} , and ε_{ij} . Thus, we can inversely calculate C_{ij} and e_{ij} from a given ε_{ij} and measured resonance frequencies f_i by solving stationary point of the Lagrangian L ,

$$L = \frac{1}{2}(S_I C_{IJ} S_J - \phi_{,m} \varepsilon_{mn} \phi_{,n} + 2\phi_{,m} e_{mJ} S_J - \rho \omega^2 u_i u_i). \quad (3)$$

Here, S denotes the engineering strain in contracted notation. ρ and ω show the mass density and the angular frequency, respectively. For the inverse calculation, the displacement u_i and the electric potential ϕ are expanded by Legendre polynomials of the order of 18 and Eq. (3) is numerically solved with the Rayleigh-Ritz method.

The temperature dependence of free vibration resonance frequencies f_i is measured by a tripod-type RUS measurement system.²⁶ The RUS unit and specimen are set into a cryogenic chamber, and low temperature measurements have been carried out from 5 K to ambient temperature with $\Delta T = 5$ K. Temperature inaccuracy is approximately ± 0.1 K throughout the study. Free vibration resonance spectra have been obtained from 0.3 to 1.1 MHz, and the resonance frequencies are determined by the Lorentzian-function fitting

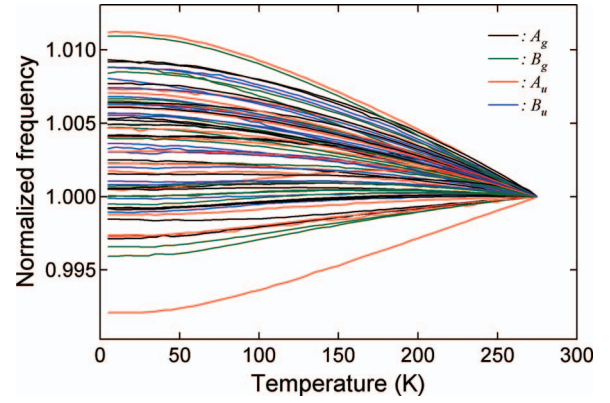


FIG. 1. (Color) Temperature dependence of free vibration resonance frequencies obtained by RUS. Resonance frequencies are normalized by their ambient temperature values and classified into four irreducible representations: A_g , B_g , A_u , and B_u .

procedure; more than 60 peaks are obtained at each temperature step. The average rms error between experimental and theoretical resonance frequencies is approximately 0.15%. The symmetry of the macroscopic free vibration of a parallelepiped-shaped α -quartz specimen is given by the point group C_{2h} , which has four irreducible representations: A_g , B_g , A_u , and B_u .²⁹ Resonance frequencies are unambiguously matched by comparing surface displacement distributions measured by laser-Doppler interferometer with those of calculations.^{11,26}

III. EXPERIMENTAL RESULTS

Figure 1 shows a temperature dependence of normalized resonance frequencies. We find no distinctive difference due to the macroscopic free vibration symmetries. Most frequency changes fall into the range of 1% to -0.5% and some modes show extremely high temperature stability with only $\pm 0.02\%$ change. Ohno reported an exchange of vibration symmetry if resonance frequencies of two different modes approach each other.³⁰ According to Ohno, this phenomenon is interpreted as the mode coupling induced by lattice defects such as orientational and/or chiral twinings.¹ A crystallographic misorientation of the specimen also causes this effect. As seen from Fig. 1, however, we did not find such effect over the entire modes, indicating that a combination of defects and orientation errors is negligible in this work.

Table I summarizes the low temperature elastic constants C_{ij} , bulk modulus B , and piezoelectric coefficients e_{ij} of the α -quartz. Θ_D represents the acoustic Debye temperature calculated from the complete C_{ij} set by numerically solving the Christoffel equation. From Table I, we see that most C_{ij} changes by only a few percent while the changes in C_{12} and e_{ij} are notable; C_{12} increases by about 30% and e_{ij} decreases

TABLE I. Elastic constants C_{ij} , piezoelectric coefficients e_{ij} , and acoustic Debye temperature Θ_D of α -quartz at 275 and 5 K. Θ_D is calculated from the complete set of C_{ij} by numerically solving the Christoffel equation. The units are GPa for C_{ij} and B , C/m^2 for e_{ij} , and K for Θ_D , respectively.

T (K)	C_{11}	C_{12}	C_{13}	C_{14}	C_{33}	C_{44}	C_{66}	B	e_{11}	e_{14}	Θ_D
275	86.76	7.06	11.90	-17.98	105.41	58.27	39.85	37.37	0.149	-0.057	(588.1)
5	87.65	9.42	12.80	-17.83	107.65	59.60	39.12	38.75	(0.066)	(-0.026)	590.1

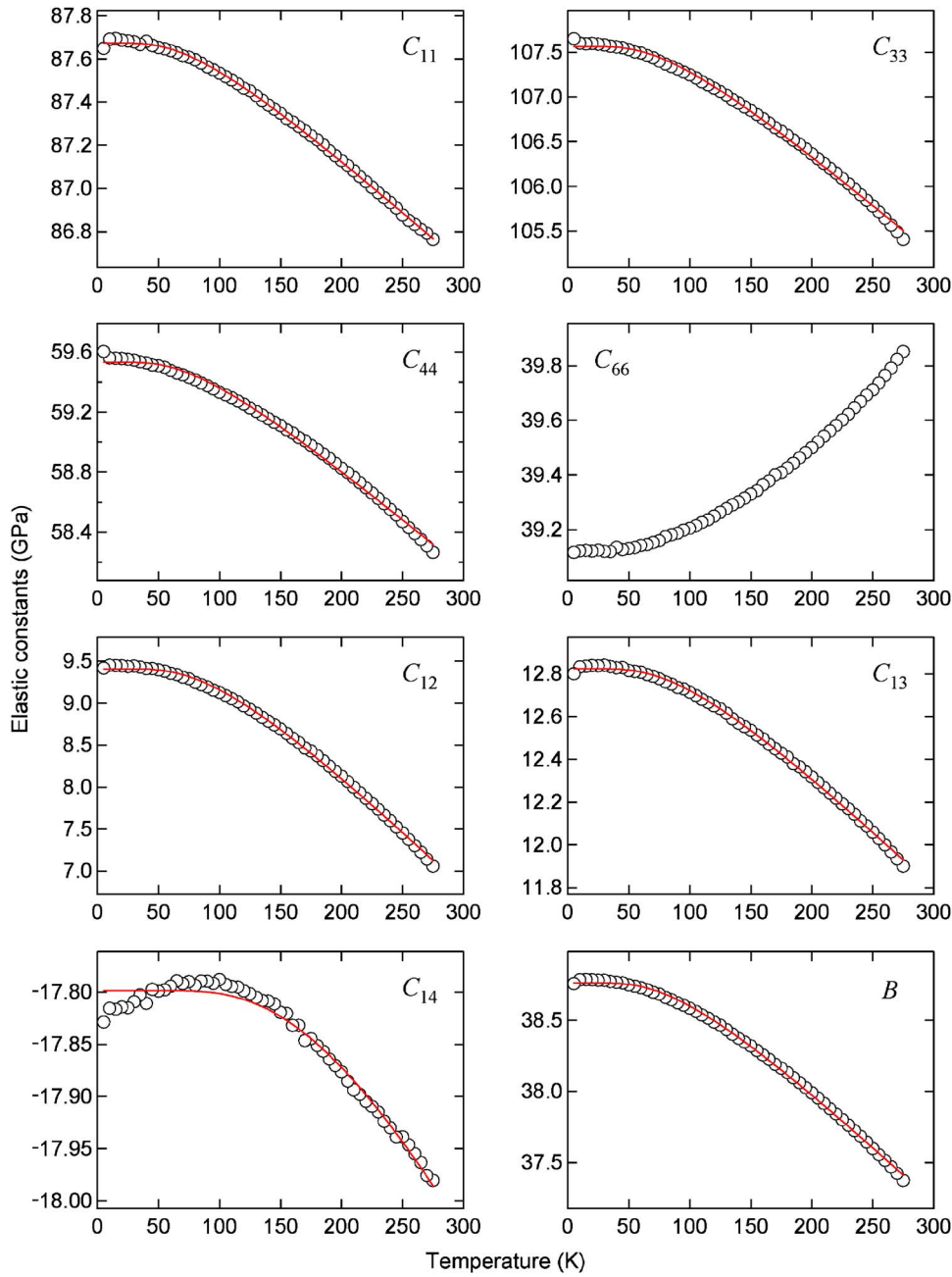


FIG. 2. (Color online) Temperature dependence of elastic constants C_{ij} and bulk modulus B . C_{66} continuously softens throughout the temperature range, and C_{14} shows weak softening below 100 K. Solid curves in the figures show the least-squares fitting results to Varshni's function (Ref. 32).

by a factor of 0.5. The violation of the Cauchy relation, $C_{12}=C_{66}$, $C_{13}=C_{55}(=C_{44})$, is still significant at 5 K. Figure 2 presents the temperature dependence of elastic constants C_{ij} . Most elastic constants show monotonic elastic stiffening, while C_{66} shows continuous softening upon cooling. Following the previous work,¹ the temperature dependence of elastic constants $C_{ij}(T)$ is analyzed by means of the third-order Taylor series expansion,

$$\frac{\Delta C_{ij}}{C_{ij}(0)} = T_{C_{ij}}^{(1)} \Delta T + T_{C_{ij}}^{(2)} (\Delta T)^2 + T_{C_{ij}}^{(3)} (\Delta T)^3, \quad (4)$$

with

$$T_{C_{ij}}^{(n)} = \frac{1}{n! C_{ij}(0)} \left. \frac{\partial^n C_{ij}}{\partial T^n} \right|_{T=T_0}, \quad (5)$$

where $\Delta C_{ij} = C_{ij} - C_{ij}(0)$ and $\Delta T = T - T_0$. $C_{ij}(0)$ represents the elastic constants at T_0 ($=275$ K). The temperature coeffi-

icients $T_{C_{ij}}^{(n)}$ are summarized in Table II. Present results showed reasonable agreements with previous works on the first-order coefficients $T_{C_{ij}}^{(1)}$, while slight inconsistencies have been confirmed in the higher-order terms.¹ The discrepancies can be attributed to the difference in measurement tempera-

TABLE II. Temperature coefficients of elastic constants $T_{C_{ij}}^{(n)}$ defined in Eqs. (4) and (5).

	$T_{C_{ij}}^{(1)}$ ($10^{-6}/\text{K}$)	$T_{C_{ij}}^{(2)}$ ($10^{-9}/\text{K}^2$)	$T_{C_{ij}}^{(3)}$ ($10^{-12}/\text{K}^3$)
C_{11}	-53.9 ± 0.6	50.8 ± 7.2	390.5 ± 19.6
C_{12}	-2200 ± 11.7	-2141.1 ± 133	5079.4 ± 361
C_{13}	-500.7 ± 5.9	-365.2 ± 67.3	1531.1 ± 183
C_{14}	83.9 ± 1.8	29.5 ± 20.8	-602.9 ± 56.4
C_{33}	-136.5 ± 1.3	-206.4 ± 14.8	31.1 ± 40.2
C_{44}	-146.2 ± 0.9	-243.3 ± 10.8	-49.8 ± 29.2
C_{66}	136.2 ± 1.0	245.2 ± 11.3	-24.5 ± 30.8

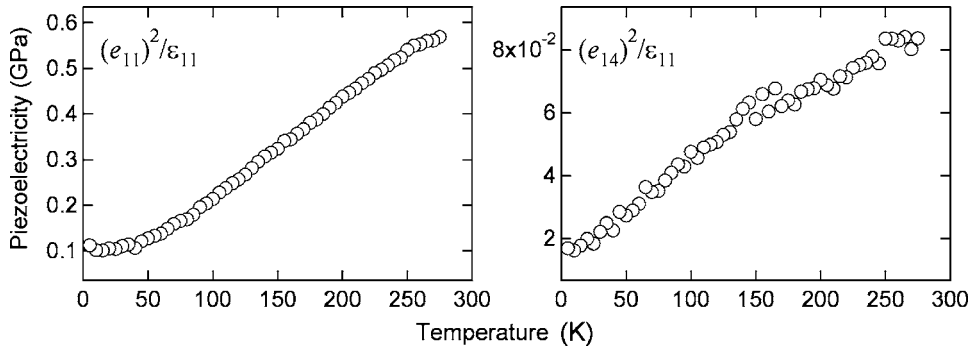


FIG. 3. Temperature dependence of piezoelectricity coefficients. Note that we plot e_{ij}^2/ϵ_{11} since it gives the same unit with C_{ij} and since e_{ij} and ϵ_{ij} are inseparable with each other.

ture range between the present (5–275 K) and previous works (218–363 K). Thus, the quantitative consistency of $T_{C_{ij}}^{(1)}$ supports our measurement accuracies and the present higher-order terms would be useful for theoretical and/or practical applications at low temperatures.

Let us discuss the low temperature lattice dynamics of α -quartz from $C_{ij}(T)$ behaviors. The solid curves in Fig. 2 show the least-squares fitting result to Varshni's function; $C_{ij}(T) = C_{ij}^0 - s/[\exp(t/T) - 1]$, where t represents the Einstein temperature Θ_E .³¹ The estimated t becomes $t_{C11}=228$ K, $t_{C33}=240$ K, $t_{C12}=289$ K, $t_{C13}=280$ K, $t_{C44}=236$ K, $t_B=270$ K, and $t_{C14}=637$ K. Compared with the original definition of Θ_E ($=0.75\Theta_D=443$ K), the temperature dependence of $C_{14}(T)$ is obviously far from being usual because the estimated Einstein temperature is too high. The zone-center mode mean Grüneisen parameter γ , estimated from the temperature slope of the bulk modulus dB/dT , becomes 1.15.³¹

Piezoelectric coefficients e_{ij} also provide attracting material properties. Our measurement reveals that both e_{11}^2/ϵ_{11} and e_{14}^2/ϵ_{11} monotonically decreases with temperature (see Fig. 3). As is well known, the piezoelectricity appears by the loss of inversion symmetry in the point group operation (20 of 32 point groups show this effect). Continuous decreasing of e_{ij} therefore, suggests the formation of internal strain associated with macroscopic thermal contraction. As mentioned above, α -quartz is constructed from SiO_4 tetrahedra sharing their corners with each other. Since the covalent bond in the tetrahedron is sufficiently high, low temperature volume contraction will be mainly caused by the rigid body rotation of the tetrahedra. Such a microscopic picture has been confirmed by the previous work and a high temperature α - β phase transition is driven by a soft mode phonon associated with the rotation.³³ The internal strain can be ascribed to the static optical-mode phonons,³⁴ which disturb the crystal field around ions and will eventually affect the piezoelectricity.

Another notable feature is found between C_{66} and e_{11}^2/ϵ_{11} ; namely, these independent coefficients show an almost linear relation especially below 200 K. The Pearson product-moment correlation coefficient becomes 0.98, which is remarkably close to unity and represents a strong correlation between these coefficients. The correlation suggests that a single mode internal strain affects both C_{66} and e_{11}^2/ϵ_{11} simultaneously. In the next section, the origins of the unusual elastic behaviors and the correlation between C_{66} and e_{11} will be discussed from a group theoretical lattice dynamics perturbation approach.

IV. DISCUSSION

A. Normal modes of α -quartz at the Γ point

First of all, we briefly summarize the crystallography of α -quartz from a group theoretical point of view. In the trigonal unit cell, six O atoms are located at the following 6c Wyckoff positions: (1) $[x, y, z]$, (2) $[-y, x-y, z+2/3]$, (3) $[-x+y, -x, z+1/3]$, (4) $[-x, -y, -z]$, (5) $[x-y, -y, -z+1/3]$, and (6) $[-x, -x+y, -z+2/3]$.³⁵ Since these are general positions, the vectors (1)–(6) represent the symmetry operations G_i in the space group. The group elements can be divided into three classes C_i : $C_1=\{G_1\}$, $C_2=\{G_2, G_3\}$, and $C_3=\{G_4, G_5, G_6\}$, representing identical, screw, and π -rotation operations, respectively. Three Si atoms are located at the 3b site, one of which is left unmoved by an operation in C_3 .

It is useful to employ normal modes to describe lattice vibration. Elastic and piezoelectric properties are related to long-wavelength vibrations (or wave number $k=0$ in a reciprocal lattice); we thus restrict our considerations to the center of the Brillouin zone (Γ point). Then, the space group of the α -quartz $P3_221$ becomes isomorphic to the point group of D_3 . The character table and basis functions of the D_3 group are summarized in Table III.³⁶ It has three irreducible representations, where A_1 is Raman active, A_2 is infrared active, and both are active in the E mode, as expected from the basis functions.

The displacement vectors in the α -quartz unit cell have $3 \times 9 = 27$ degrees of freedom. Expressing the number of atoms that are left unmoved by an operator G_i by N_i , it becomes $N_1=9$, $N_{2,3}=0$, and $N_{4,5,6}=1$. On the other hand, the character χ_i of an operation G_i is simply given by $\chi_i=1+2\cos\theta$, where θ represents the rotation angle of G_i .³⁵ Then, the characters of the 27 dimensional displacements $\chi=N_i\chi_i$ become

TABLE III. Character table and basis functions for the point group of D_3 . The basis functions are defined to a $x_1x_2x_3$ -Cartesian coordinate system and calculated to the first- and second-order polynomials by projection operations (Ref. 36).

	C_1	C_2	C_3	Basis function
A_1	1	1	1	$x_3^2, x_1^2+x_2^2$
A_2	1	1	-1	x_3
E	2	-1	0	$\{x_1, x_2\}, \{x_2x_3, -x_3x_1\}$ $\{x_1x_2, (x_1^2-x_2^2)/2\}$

$$\chi = 27G_1 - G_4 - G_5 - G_6. \quad (6)$$

Note that χ includes the following translational motions: $\chi = 3G_1 - G_4 - G_5 - G_6$. Now, we reduce Eq. (6) to a direct sum of irreducible representations. From a great orthogonality theorem, coefficient q_α for an irreducible representation α is given by³⁶

$$q_\alpha = \frac{1}{g} \sum_G \chi^\alpha(G)^* \chi^\alpha(G), \quad (7)$$

where g is the order of group and the asterisk represents a complex conjugate. By Eq. (7) and Table II, Eq. (6) can be decomposed into the following form:

$$\chi = (A_2 + E) + 4(A_1 + A_2 + 2E). \quad (8)$$

The term in the first parentheses represents the three acoustic modes, and that in the second shows other 24 optical modes. The optical mode includes all three symmetries, while only A_2 and doubly degenerated E are included in the acoustic mode. The totally symmetric A_1 acoustic mode is forbidden at the Γ point.

B. Effect of internal strain on elastic constants and piezoelectric coefficients

We discuss the effect of internal strains on elastic constants C_{ij} and piezoelectric coefficients e_{ij} from a group theoretical lattice dynamics approach. By means of a perturbation analysis for a long-wavelength equation of motion,³⁷ Miller and Axe introduced a second rank tensor $F_{\alpha\gamma}(j)$ to define the coefficient of the normal optical-mode vibration j .²⁷ By using $F_{\alpha\gamma}(j)$, they formulated the effect of the optical-mode-type internal strain on elastic constants and piezoelectric coefficients as follows:

$$C_{\alpha\gamma,\mu\delta} = - \sum_j \frac{1}{\omega_e^2(j)} F_{\alpha\gamma}(j) F_{\mu\delta}(j), \quad (9)$$

$$e_{\mu,\alpha\gamma} = - \sum_j \frac{1}{\omega_e^2(j)} P_\mu(j) F_{\alpha\gamma}(j), \quad (10)$$

where $C_{\alpha\gamma,\mu\delta}$ and $e_{\mu,\alpha\gamma}$ show the internal strain part of the elastic constants and of the piezoelectric coefficients, respectively. $\omega_e(j)$ and $P_\mu(j)$ represent the vibration frequency and polarization of mode j . Since $F_{\alpha\gamma}(j)$ and $P_\mu(j)$ transform as second and first rank tensors by a given point group operation, Eqs. (9) and (10) represent that only the Raman active mode contributes to the internal strain part of elastic constants and only modes that are both Raman and infrared active contribute to piezoelectric coefficients. Note that the effect of the acoustic mode is taken to vanish in the formula.

Let us consider the transformations of $F_{\alpha\gamma}(j)$ and $P_\mu(j)$ in the present D_3 group under the $x_1x_2x_3$ -Cartesian coordinate system. With the help of basis functions (see Table III), nonvanishing $F_{\alpha\gamma}(j)$ components for the A_1 mode $F_{\alpha\gamma}(A_1)$ are $F_{11}(A_1) = F_{22}(A_1)$ and $F_{33}(A_1)$. Similarly, E allows $F_{23}(E)$, $F_{31}(E)$, $F_{12}(E)$, $F_{11}(E) = -F_{22}(E)$. On the other hand, the nonvanishing polarization $P_\mu(j)$ for the A_2 mode is $P_3(A_2)$, and those for the E mode are $P_1(E)$ and $P_2(E)$.

The full fourth-rank tensor notation of C_{66} is C_{1212} so that $F_{12}(E)$ doubly contributes to the coefficient. As seen from Eq. (8), the E symmetry is included in the optical mode and $F_{12}(j)$ exists only in E . Thus, the low temperature softening in C_{66} can be realized by the effect of the optical-phonon-type internal strain, which has a symmetry of E . On the other hand, piezoelectric coefficients are affected only by the E mode since it requires both Raman and infrared active. From Eq. (2), nonzero components of the third rank tensor are $e_{111} = -e_{122} = -e_{212}$ ($= \pm e_{11}$) and $e_{123} = -e_{233}$ ($= \pm e_{14}$). Thus, the possible combinations of $P_\mu(E)F_{\alpha\gamma}(E)$ are $P_1(E)F_{11}(E)$, $P_1(E)F_{22}(E)$, and $P_2(E)F_{12}(E)$ for e_{11} , and $P_1(E)F_{23}(E)$ and $P_2(E)F_{31}(E)$ for e_{14} . Clearly, $F_{12}(E)$ contributes to e_{11} as C_{66} , too. This would explain the strong correlation between C_{66} and e_{11}^2/ϵ_{11} . Similarly, we also see the effect of $F_{12}(E)$ on the unusual softening in C_{14} below 100 K. From Eq. (1), $C_{14} = C_{26} = C_{2212}$ so that the contributing coefficients are $F_{22}(E)$ and $F_{12}(E)$. Thus, the effect of $F_{12}(E)$ on C_{14} is straightforward.

Finally, we mention the A_2 mode internal strain. The present results cannot access this mode since it does not influence C_{ij} and e_{ij} . Thus, the existence of the thermal contraction induced A_2 mode internal strain is unclear. Here, theoretical calculations such as molecular dynamics would be useful. The present low temperature C_{ij} and e_{ij} are helpful to evaluate the accuracy of these theoretical calculations.

V. CONCLUSIONS

In summary, we investigated the low temperature elastic constants C_{ij} and piezoelectric coefficients e_{ij} of the α -quartz single crystal using the RUS/LDI method. Conclusions of the present study are summarized as follows.

- (i) Most elastic constants showed monotonic stiffening, while C_{66} continuously softens with decreasing temperature.
- (ii) The elastic constant change between 5 K and ambient temperature is only a few percent while C_{12} increases by a factor of 1.3 upon cooling.
- (iii) Cauchy relations are severely violated throughout the present temperature range.
- (iv) Compared with ambient temperature values, piezoelectric coefficients, e_{11} and e_{14} , decrease by about a factor of 0.5 at 5 K. Such notable decrease in e_{ij} suggests the formation of internal strains associated with macroscopic thermal contraction.
- (v) We find a strong correlation between C_{66} and e_{11}^2/ϵ_{11} especially below 200 K. The group theoretical lattice dynamics analysis revealed that the elastic softening found in C_{66} and C_{14} and the correlation between C_{66} and e_{11}^2/ϵ_{11} can be explained from the formation of an optical-mode-phonon-type internal strain, which has a doubly degenerated E symmetry in the point group of D_3 .

¹M. Levy, H. E. Bass, and R. R. Stern, *Handbook of Elastic Properties of Solids, Liquids and Gases* (Academic, San Diego, 2001), Vol. II.

²E. Gregoryanz, R. J. Hemley, H. K. Mao, and P. Gillet, *Phys. Rev. Lett.* **84**, 3117 (2000).

- ³R. Bechmann, Phys. Rev. **110**, 1060 (1958).
- ⁴R. Bechmann, A. D. Ballato, and T. J. Lukaszek, Proc. IRE **50**, 1812 (1962).
- ⁵I. Koga, M. Aruga, and Y. Yoshinaka, Phys. Rev. **109**, 1467 (1958).
- ⁶B. J. James, in the *Proceedings of the 42nd Annual Frequency Control Symposium* (IEEE, Baltimore, 1988), p. 146.
- ⁷R. K. Cook and P. G. Weissler, Phys. Rev. **80**, 712 (1950).
- ⁸J. Kushibiki, I. Takanaga, and S. Nishiyama, IEEE Trans. Ultrason. Ferroelectr. Freq. Control **49**, 125 (2002).
- ⁹H. J. McSkimin, P. Andreatch, and R. N. Thurston, J. Appl. Phys. **36**, 1624 (1965).
- ¹⁰J. V. Atanasoff and P. J. Hart, Phys. Rev. **59**, 85 (1941).
- ¹¹H. Ogi, T. Ohmori, N. Nakamura, and M. Hirao, J. Appl. Phys. **100**, 053511 (2006).
- ¹²Y. Ma and S. H. Garofalini, Phys. Rev. B **73**, 174109 (2006).
- ¹³J. D. Axe and G. Shirane, Phys. Rev. B **1**, 342 (1970).
- ¹⁴U. T. Hochli and J. F. Scott, Phys. Rev. Lett. **26**, 1627 (1971).
- ¹⁵N. Choudhury and S. L. Chaplot, Phys. Rev. B **73**, 094304 (2006).
- ¹⁶R. J. Hemley, A. P. Jephcoat, H. K. Mao, L. C. Ming, and M. H. Manghnani, Nature (London) **334**, 52 (1988).
- ¹⁷L. E. McNeil and M. Grimsditch, Phys. Rev. Lett. **68**, 83 (1992).
- ¹⁸H. Kimizuka, S. Ogata, J. Li, and Y. Shibutani, Phys. Rev. B **75**, 054109 (2007).
- ¹⁹N. Keskar and J. R. Chelikowsky, Nature (London) **358**, 222 (1992).
- ²⁰J. F. Scott and S. P. S. Porto, Phys. Rev. **161**, 903 (1967).
- ²¹M. E. Striefler and G. R. Barsh, Phys. Rev. B **12**, 4553 (1975).
- ²²J. H. Demarest, J. Acoust. Soc. Am. **49**, 768 (1971).
- ²³I. Ohno, J. Phys. Earth **24**, 355 (1976).
- ²⁴A. Migliori and J. Sarro, *Resonant Ultrasound Spectroscopy* (Wiley Interscience, New York, 1997).
- ²⁵R. G. Leisure and F. A. Willis, J. Phys.: Condens. Matter **9**, 6001 (1997).
- ²⁶H. Ogi, K. Sato, T. Asada, and M. Hirao, J. Acoust. Soc. Am. **112**, 2553 (2002).
- ²⁷P. B. Miller and J. D. Axe, Phys. Rev. **163**, 924 (1967).
- ²⁸A. F. Wright and M. S. Lehmann, J. Solid State Chem. **36**, 371 (1981).
- ²⁹E. Mochizuki, J. Phys. Earth **35**, 159 (1987).
- ³⁰I. Ohno, J. Phys. Earth **43**, 157 (1995).
- ³¹H. Ledbetter, Phys. Status Solidi B **181**, 81 (1994).
- ³²Y. P. Varshni, Phys. Rev. B **2**, 3952 (1970).
- ³³M. B. Smirnov and A. P. Mirgorodsky, Phys. Rev. Lett. **78**, 2413 (1997).
- ³⁴M. E. Simon and C. M. Varma, Phys. Rev. Lett. **86**, 1781 (2001).
- ³⁵T. Hahn, *The International Tables for Crystallography A: Space-Group Symmetry* (Springer, Dordrecht, 2005).
- ³⁶T. Inui, Y. Tanabe, and Y. Onodera, *Group Theory and Its Applications in Physics* (Springer-Verlag, Berlin, 1996).
- ³⁷M. Born and K. Huang, *Dynamical Theory of Crystal Lattice* (Clarendon, Oxford, 2002).